Wide-angle elastic scattering and color randomization

Michael G. Sotiropoulos*

Physics Department, University of Southampton, Southampton, SO17 1BJ, United Kingdom

(Received 2 January 1996)

Baryon-baryon elastic scattering is considered in the independent scattering (Landshoff) mechanism. It is suggested that for scattering at moderate energies direct and interchange quark channels contribute with equal color coefficients because the quark color is randomized by soft gluon exchange during the hadronization stage. With this assumption, it is shown that the ratio of cross sections $R_{\bar{p}p/pp}$ at a c.m. angle $\theta = 90°$ decreases from a high energy value of $R_{\bar{p}p/pp} \approx 1/2.7$, down to $R_{\bar{p}p/pp} \approx 1/28$, compatible with experimental data at moderate energies. This sizable fall in the ratio seems to be characteristic of the Landshoff mechanism, in which changes at the quark level have a strong effect precisely because the hadronic process occurs via multiple quark scatterings. The effect of color randomization on the angular distribution of proton-proton elastic scattering and the cross section ratio $R_{np/pp}$ is also discussed. [S0556-2821(96)00811-9]

PACS number(s): 13.60.Fz, 13.85.Dz

I. INTRODUCTION

The analysis of exclusive hadronic processes within the framework of perturbative QCD (PQCD) remains conceptually as well as computationally challenging. In the case of hadronic elastic scattering at high energy and wide c.m. angle, the formalism for the treatment of the amplitude has been developed in the kinematic region of momentum transfer $|t|$ much larger than the hadronic mass scales. The long distance dynamics of the hadronic bound state factorize from the short distance scattering of the constituent quarks. Specifically, for baryon-baryon elastic scattering the amplitude takes the factorized form [1]

$$\mathcal{A}(s,t;h_i) = \int \prod_{i=1}^{4} [dx]_i \phi_i(x_{m,i}, \lambda_{m,i}, h_i; \mu)$$
$$\times M_H(\hat{s}_{ij}, \lambda_{m,i}; \mu), \qquad (1)$$

where $i,j = 1,2,3,4$ are the baryon labels, $m,n = 1,2,3$ are the constituent quark labels, and

$$\int [dx]_i \equiv \int_0^1 dx_{1,i} dx_{2,i} dx_{3,i} \delta\left(1 - \sum_{n=1}^{3} x_{n,i}\right).$$

The hard scattering amplitude $M_H(\hat{s}_{ij}, \lambda_{m,i}; \mu)$ describes the scattering of nearly collinear constituent quarks with helicities $\lambda_{m,i}$. It depends on the quark invariants $\hat{s}_{ij}$ but not on the hadronic mass scales. At lowest order in α_s, M_H is equal to the Born amplitude with, in principle, calculable higher order corrections. The quark distribution amplitudes $\phi_i(x_{m,i}, \lambda_{m,i}, h_i; \mu)$ describe the three-valence quark component of the baryon wave function with helicity h_i and it is evaluated at factorization scale $\mu^2 = O(|t|)$, with calculable $\ln t$ corrections. In the single hard scattering mechanism, where all constituents scatter together in a small space-time region, the calculation of M_H at lowest order, $O(\alpha_s^5(\mu))$, requires the evaluation of approximately 300 000 distinct

tree graphs for $6q \to 6q$ scattering [2]. Moreover, the inclusion of higher order radiative corrections and the implementation of the factorization of infrared singularities make this approach unyielding. Alternatively, and long before the above complications were studied in such detail, two distinct scattering mechanisms had been considered. The first is the quark interchange model (QIM) [3], in which the scattering is assumed to proceed via the exchange of a pair of quarks between the scattering hadrons. The second is the independent scattering (Landshoff) mechanism [4], in which the quarks from each initial hadron scatter pairwise and independently up to logarithmic radiative corrections. From the PQCD point of view, both QIM and Landshoff-type diagrams originate as particular pinch singularities of the single hard scattering diagrams, although the two sets are distinct [5].

The experimental studies of wide-angle elastic scattering at moderate energies suggest that the process is mainly driven by the QIM mechanism [6,7]. In particular, QIM is consistent with the dimensional counting scaling behavior of the elastic baryon cross section

$$\frac{d\sigma^{BB}}{dt} \sim \frac{1}{s^{10}} f(\theta), \qquad (2)$$

its dependence on the c.m. angle θ as given by the function $f(\theta)$, as well as its flavor and crossing properties manifested by the cross section ratios such as

$$R_{\bar{p}p/pp}(s,\theta) = \frac{d\sigma^{\bar{p}p}/dt}{d\sigma^{pp}/dt}. \qquad (3)$$

On the other hand, the Landshoff mechanism seems to have negligible contribution to the elastic scattering. This fact remains a puzzle since, within PQCD, independent quark scattering, being $O(\alpha_s^3(\mu))$ modulo radiative corrections, is anticipated to contribute. Indeed, Botts [8] has studied numerically the Landshoff mechanism with Sudakov-resummed radiative corrections. With reasonable choices for the end point and infrared cutoff parameters, he has con-

---

*Electronic address: mgs@hep.phys.soton.ac.uk

cluded that Landshoff-type contributions to the cross section are non-negligible and must be included in the phenomenology of elastic scattering.

In this paper we consider the above puzzle. Specifically, we reexamine the Landshoff mechanism and study to what extent it can account for certain features of the elastic baryon cross sections such as their angular dependence and the ratios $R_{\bar{p}p/pp}(s,\theta)$ and $R_{np/pp}(s,\theta)$ in the moderate energy regime where measurements are available. Recent experiments at the BNL Alternate Gradient Synchrotron (AGS) [7] have measured $R_{\bar{p}p/pp} \approx 1/40$ at $\sqrt{s}=3.59$ GeV and $\theta=90°$. This measurement is near the beginning of the scaling region as given by Eq. (2). Of course, the energy here is not high enough for a fully self-consistent perturbative treatment of the process in terms of independent hard scatterings. Nevertheless, in a constituent quark model, $R_{\bar{p}p/pp}$ is largely determined by the flavor flows, i.e., the number of possible routings of the quarks among the participating hadrons, and the color factors arising from combining the color structure of the hard scatterings with the color singlet external hadrons. Expecting this ratio to be less sensitive than the elastic cross section itself to the factorization assumptions, we compute it using the formalism of PQCD. In a sense, the treatment presented below supplies a QCD-motivated model which realizes the observation that elastic scattering is dominated by quark interchange. We emphasize again that order by order in perturbation theory the diagrams contributing to the QIM and Landshoff mechanisms are topologically different as far as gluon exchange is concerned. However, the Landshoff mechanism, which is considered here, does contain contributions in which quarks are interchanged between the scattering hadrons, as explained further in the following section.

Our starting point is the factorized form of the elastic amplitude in the Landshoff mechanism, which we briefly review in Sec. II. In Sec. III the idea of color randomization is presented and its effect on the crossing properties of the elastic amplitude is illustrated by considering a toy model of scalar quarks. The main point is that there is always soft gluon exchange among the constituent quarks in the initial and final states which cannot be factored into the hadronic wave functions and mixes the quark color. In the asymptotic high energy regime, where soft radiation can be treated perturbatively, it is possible to relate the color of the quarks at the hadronization region with their color at the hard scattering region by computing color traces order by order in α_s. But for moderate energies, where a perturbative expansion for soft gluon exchange is not self-consistent, we suggest that the effect of soft radiation is to decorrelate the color of the constituent quarks at hadronization from the color they have when they participate in the hard scatterings. In other words, by the time the quarks enter the hard scattering region, their color has been randomized by soft gluon exchange. We express this color randomization by requiring that all quark channel combinations, i.e. direct (ttt), total interchange (uuu), and single and double interchanges (ttu, tuu), contribute with the same color coefficients when summed in the calculation of the elastic proton-proton amplitude. In Sec. IV we compute the pp, $\bar{p}p$, and np elastic amplitudes in the helicity basis and at lowest order in α_s for the hard scatterings. At asymptotically high energies, we expect color flow to be dominated by lowest order contribu-
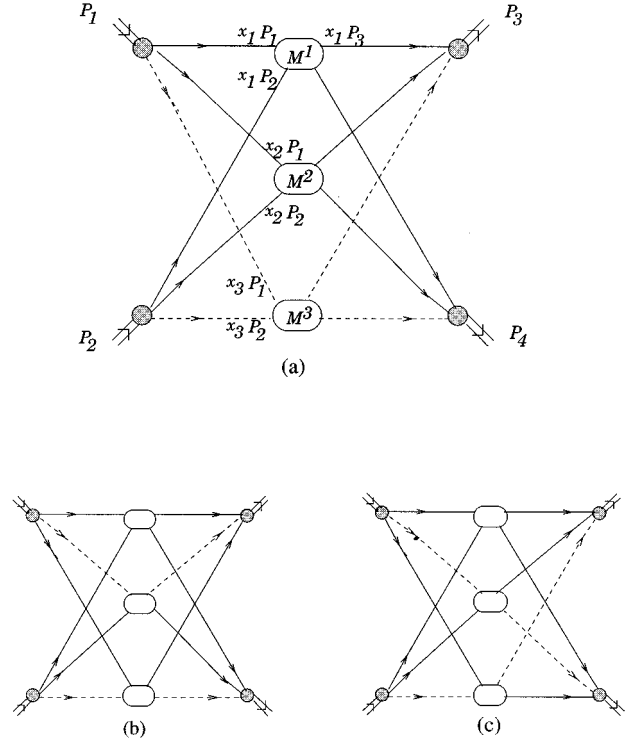

FIG. 1. Proton-proton elastic scattering in the Landshoff mechanism and inequivalent flavor routings. The dashed lines represent the d quarks. All momenta flow from left to right.

tions. This gives an asymptotic ratio $R_{\bar{p}p/pp}^{\text{as}} \approx 1/2.7$ at $\theta=90^0$. In the color randomization model suggested for sub-asymptotic energies, we find $R_{\bar{p}p/pp}^{\text{rand}} \approx 1/28$. The effect of color randomization on the angular distribution of proton-proton elastic scattering and the ratio $R_{np/pp}$ is also considered. We end by discussing these results.

II. THE LANDSHOFF MECHANISM IN PQCD

The structure of the elastic amplitude via independent quark scatterings [4] is shown in Fig. 1 for $pp \rightarrow pp$. Only the three-valence quark part of the proton wave function is considered and M^1, M^2, and M^3 represent on-shell quark-quark scatterings. In leading twist factorization, the hard scatterings M^m, $m=1,2,3$, depend only on the longitudinal quark momenta $x_{m,i}P_i$, that scale with $\sqrt{s}$ in the proton c.m. frame. The longitudinal momentum fractions are characterized by both a hadronic label i and a scattering label m. The kinematics of on-shell q-q scattering requires that quarks participating in the same hard scattering have equal momentum fractions, i.e.,

$$x_{1,i}=x_1 \geq 0, \quad x_{2,i}=x_2 \geq 0, \quad x_{3,i}=1-x_1-x_2 \geq 0, \quad (4)$$

for every $i=1,2,3,4$ up to $O(1/\sqrt{s})$ corrections. Dependence on transverse momentum and hadronic mass scales resides in the hadronic wave functions.

The hard scatterings lie along the spacelike direction η^μ, perpendicular to the scattering plane. This is the line of intersection of the Lorentz contracted wave functions of the incoming and outgoing protons. We denote by b_m the posi-

tions of the hard scatterings M^m along the η^μ direction and by $\widetilde{b}_m$ their mutual transverse separations defined as

$$\widetilde{b}_1 = b_2 - b_3, \quad \widetilde{b}_2 = b_1 - b_3, \quad \widetilde{b}_3 = \widetilde{b}_2 - \widetilde{b}_1. \quad (5)$$

The three-quark component of the proton wave function is obtained as a Fourier transform of the three-quark operator [9]

$$Y_{\alpha\beta\gamma}(k_1,k_2;P,h) = \frac{(\sqrt{2}E)^{1/2}}{N_c!} \int \frac{d^4 y_1}{(2\pi)^4} e^{ik_1\cdot y_1} \frac{d^4 y_2}{(2\pi)^4} e^{ik_2\cdot y_2}$$
$$\times \langle 0|T[u_\alpha^a(y_1)u_\beta^b(y_2)d_\gamma^c(0)]|P,h\rangle \epsilon_{abc}, \quad (6)$$

where E is the energy of the fast moving proton and h its helicity. The wave function is decomposed in terms of valence quark spinors with definite helicity. Defining the dimensionless structures [10]

$$\mathcal{M}_{\alpha\beta\gamma}^{(1)} = (E_1 E_2 E_3)^{-1/2} u_\alpha(k_1,+) u_\beta(k_2,-)$$
$$\times d_\gamma(P-k_1-k_2,+),$$

$$\mathcal{M}_{\alpha\beta\gamma}^{(2)} = (E_1 E_2 E_3)^{-1/2} u_\alpha(k_1,-) u_\beta(k_2,+)$$
$$\times d_\gamma(P-k_1-k_2,+), \quad (7)$$

$$\mathcal{M}_{\alpha\beta\gamma}^{(3)} = -(E_1 E_2 E_3)^{-1/2} u_\alpha(k_1,+) u_\beta(k_2,+)$$
$$\times d_\gamma(P-k_1-k_2,-),$$

where E_1, E_2, and E_3 are the energies of the two u quarks and the d quark, respectively, we obtain the helicity decomposition of the wave function. In impact parameter ($\widetilde{b}$-) space and for $h=+$ this is

$$\widetilde{Y}_{\alpha\beta\gamma}(x_1,x_2,x_3,\widetilde{b}_1,\widetilde{b}_2;h=+)$$
$$= \frac{2^{1/4}}{8N_c!} [\mathscr{P}_{123}\mathcal{M}_{\alpha\beta\gamma}^{(1)} + \mathscr{P}_{213}\mathcal{M}_{\alpha\beta\gamma}^{(2)} + 2\mathscr{T}_{123}\mathcal{M}_{\alpha\beta\gamma}^{(3)}], \quad (8)$$

where

$$\mathscr{T}_{123} \equiv \frac{1}{2}(\mathscr{P}_{132} + \mathscr{P}_{231}), \quad (9)$$

and $\mathscr{P}_{123} \equiv \mathscr{P}(x_1,x_2,x_3;\widetilde{b}_1,\widetilde{b}_2)$ is the proton wave function projected along the η^μ direction. Its dependence on the transverse separations $\widetilde{b}_m$ can be computed perturbatively via soft gluon resummation and results in a Sudakov exponent to be specified below. The connection of $\mathscr{P}$ to the usual light-cone distribution amplitude ϕ is given in perturbation theory via

$$\mathscr{P}(x_1,x_2,x_3,\widetilde{b}_1 \to 0,\widetilde{b}_2 \to 0;\mu) = f_N(\mu)\phi(x_1,x_2,x_3;\mu)$$
$$+ O(\alpha_s(\mu)), \quad (10)$$

where $f_N(\mu)$ is an overall normalization parameter:

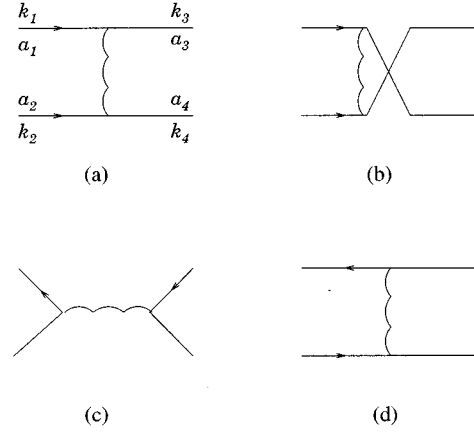$$f_N(\mu=1 \text{ GeV}) = (5.2 \pm 0.3) \times 10^{-3} \text{ GeV}^2. \quad (11)$$

FIG. 2. Exchange channels for quark-quark (a) and (b) and antiquark-quark (c) and (d) scattering.

In the asymptotic energy limit $(\mathscr{P}_{as})_{123}$ becomes symmetric upon permutation of its arguments. The asymptotic light-cone distribution amplitude is

$$\phi_{as}(x_1,x_2,x_3) = 120 x_1 x_2 x_3. \quad (12)$$

For subasymptotic energies, model-dependent ϕ's [11] are more suitable for reproducing the overall normalization of the exclusive process in which the proton participates. Finally, the color structure of the hadronic wave function is of the form ϵ_{abc}.

The main feature of the Landshoff mechanism for elastic scattering is that the hard subprocess M_H in Eq. (1) is approximated by the product of three quark amplitudes M^m. For qq scattering both t and u channels are available, Figs. 2(a) and 2(b), and for $\bar{q}q$ there are t and s channels, Figs. 2(c) and 2(d). Given the above classification, there are four channel combinations that contribute to pp or np elastic scattering, namely, the direct (ttt), Fig. 3(a), single interchange (tuu+permutations), Fig. 3(b), double interchange (tuu+permutations), and total interchange (uuu). Similarly, for $\bar{p}p$ the four possible combinations are obtained from the above by crossing from interchange to annihilation channels ($u \to s$).

The color structure of the quark scatterings can be decomposed along a two-dimensional color flow basis $(c_I)_{\{a_i\}}$, $I=1,2$. For $qq \to qq$, we choose the basis
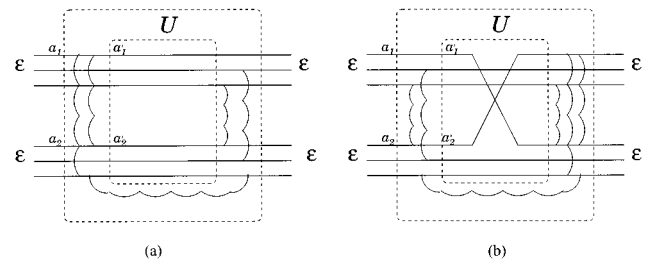

FIG. 3. Soft gluon exchange and color mixing for the direct (ttt), (a), and the single interchange (utt) channel, (b), in baryon-baryon elastic scattering. Hard gluons are not shown. Interpreted as color graphs, these diagrams represent contributions to U_{222}, (a), and U_{211}, (b).

$$(c_1)_{\{a_i\}} = \delta_{a_1 a_4} \delta_{a_2 a_3}, \quad (c_2)_{\{a_i\}} = \delta_{a_1 a_3} \delta_{a_2 a_4}. \quad (13)$$

At lowest order in α_s, the color decomposition of the direct and interchange channels is

$$(C_t)_{\{a_i\}} = (T_m)_{a_3 a_1} (T_m)_{a_4 a_2} = A_1(c_1)_{\{a_i\}} + A_2(c_2)_{\{a_i\}},$$

$$(C_u)_{\{a_i\}} = (T_m)_{a_4 a_1} (T_m)_{a_3 a_2} = A_2(c_1)_{\{a_i\}} + A_1(c_2)_{\{a_i\}}. \quad (14)$$

The color matrices T_m are normalized as $\mathrm{tr}(T_m T_n) = (1/2)\delta_{mn}$ and the color decomposition coefficients are

$$A_1 = -N_c A_2 = \frac{1}{2}. \quad (15)$$

For $\bar{q}q \to \bar{q}q$, we choose the $u \leftrightarrow s$ crossed basis

$$(\bar{c}_1)_{\{a_i\}} = \delta_{a_1 a_2} \delta_{a_3 a_4}, \quad (\bar{c}_2)_{\{a_i\}} = \delta_{a_1 a_3} \delta_{a_2 a_4}, \quad (16)$$

and the lowest order color decomposition of the direct and annihilation channels is

$$(\bar{C}_t)_{\{a_i\}} = (T_m)_{a_1 a_3} (T_m)_{a_4 a_2} = A_1(\bar{c}_1)_{\{a_i\}} + A_2(\bar{c}_2)_{\{a_i\}},$$

$$(\bar{C}_s)_{\{a_i\}} = (T_m)_{a_1 a_2} (T_m)_{a_3 a_4} = A_2(\bar{c}_1)_{\{a_i\}} + A_1(\bar{c}_2)_{\{a_i\}}, \quad (17)$$

with coefficients as in Eq. (15).

Since the amplitudes will be given in the helicity basis, we state here the two approximations made concerning helicity. The first is that the total baryon helicity is the sum of the helicities of the valence constituents, Eqs. (7) and (8). This is a consequence of leading twist factorization. Transverse momenta of the valence quarks are neglected relative to the hard scale $O(|t|)$ and the quarks are assumed to be almost collinear and moving in the direction of the parent hadron. The second approximation is helicity conservation in the quark amplitudes M^m, $m = 1,2,3$, up to $O(m_q / \sqrt{|t|})$ corrections which can be neglected for light constituents and high momentum transfers. Then, the quark amplitudes are scaleless and depend only on the c.m. angle θ. Because of helicity conservation at the baryon and quark levels, the only nonvanishing helicity baryon amplitudes are

$$\mathcal{A}(++;++) = \mathcal{A}(--;--),$$

$$\mathcal{A}(+-;+-) = \mathcal{A}(-+;-+), \quad (18)$$

$$\mathcal{A}(+-;-+) = \mathcal{A}(-+;+-).$$

The qq helicity Born amplitudes [12] for the t channel are

$$M_t(++;++) = -2g^2 \frac{s}{t} C_t = 2g^2 \frac{1}{\sin^2(\theta/2)} C_t,$$

$$M_t(+-;+-) = 2g^2 \frac{u}{t} C_t = 2g^2 \frac{\cos^2(\theta/2)}{\sin^2(\theta/2)} C_t, \quad (19)$$

$$M_t(+-;-+) = 0,$$

and, for the u channel,

$$M_u(++;++) = -2g^2 \frac{s}{u} C_u = 2g^2 \frac{1}{\cos^2(\theta/2)} C_u,$$

$$M_u(+-;+-) = 0, \quad (20)$$

$$M_u(+-;-+) = 2g^2 \frac{t}{u} C_u = 2g^2 \frac{\sin^2(\theta/2)}{\cos^2(\theta/2)} C_u.$$

The $\bar{q}q$ t channel amplitudes are as in Eqs. (19) but with opposite sign and the annihilation channel is the $s \leftrightarrow u$ crossed version of Eqs. (20), i.e.,

$$M_s(++;++) = 0,$$

$$M_s(+-;+-) = -2g^2 \frac{u}{s} \bar{C}_s = 2g^2 \cos^2(\theta/2) \bar{C}_s, \quad (21)$$

$$M_s(+-;-+) = 2g^2 \frac{t}{s} \bar{C}_s = -2g^2 \sin^2(\theta/2) \bar{C}_s.$$

So far, we have presented all the structures that determine the hadronic elastic amplitude at lowest order. Before giving its factorized form we discuss the effect of radiative corrections. In the formalism of Botts and Sterman [13], these are divided into two sets. The first set contains gluon exchange among quarks in the same hadron, which is factored into the hadronic wave functions. The second set contains soft gluon exchange among quarks from different hadrons, i.e., wave function irreducible corrections. These are factored into the color-mixing tensor $U_{\{a_i b_i c_i a'_i b'_i c'_i\}}(\tilde{b}_1, \tilde{b}_2)$, which has the perturbative expansion

$$U = \prod_{i=1}^{4} \delta_{a_i a'_i} \delta_{b_i b'_i} \delta_{c_i c'_i} + O(\alpha_s(1/\tilde{b}_m)). \quad (22)$$

Primed indices are the color indices of the quark lines entering the hard scatterings and unprimed are the color indices of the quarks at hadronization, Fig. 3. Therefore, the quark amplitudes carry primed color indices and the hadronic wave functions unprimed ones. At lowest order $O(\alpha_s^0)$, U, denoted $U^{(0)}$ below, simply describes the absence of soft gluon exchange.

Radiative corrections lead to logarithmic dependence on s/μ^2, t/μ^2, and $\tilde{b}_m^2/\mu^2$, where μ is the factorization scale. Logarithmic corrections can be resummed into exponential factors $\exp(-S_I)$, the Sudakov suppression factors. The Sudakov exponent S_I corresponding to a certain hard scattering M^m with color flow along the direction $I = 1,2$, is [14,13]

$$S_I(Q_m, \tilde{b}_m) = \frac{8 C_F}{9} \ln(Q_m/\Lambda) \ln \frac{\ln(Q_m/\Lambda)}{\ln(1/|\tilde{b}_m|\Lambda)} + (\mathrm{NL})_I, \quad (23)$$

where $Q_m^2 = O(x_m^2 |t|)$ is the hard scale of M^m and Λ is the QCD scale parameter. In the axial gauge, the leading logarithmic corrections describe the perturbative evolution of the wave function with the hard scale Q and the nonleading logarithmic corrections $(\mathrm{NL})_I$ are generated by the wave function irreducible soft gluon exchange and depend on the color flow I of the hard scattering.

We introduce the following notation. Given color tensor $C_{\{a_i, b_i, c_i\}}$, $i = 1,2,3,4$, we denote by $\mathrm{tr}_c(C)$ the contraction of the indices of C with the color structure of the baryon wave functions: i.e.,

$$\mathrm{tr}_c(C) \equiv \prod_{i=1}^{4} \sum_{a_i, b_i c_i} \epsilon_{a_i b_i c_i} C_{\{a_i, b_i, c_i\}}. \qquad (24)$$

Then the factorized form of the elastic amplitude in impact parameter space is [13]

$$\mathscr{A}(s,t;h_i) = \frac{N}{stu} \sum_f \int_0^1 \frac{dx_1 dx_2}{x_1^2 x_2^2 x_3^2} \int d\widetilde{b}_1 d\widetilde{b}_2 \mathscr{R}^{(f)}$$
$$\times \mathrm{tr}_c(U M^1 M^2 M^3) \exp(-S^1 - S^2 - S^3), \qquad (25)$$

where

$$N = \frac{\pi^6}{2(N_c!)^4} \qquad (26)$$

is a numerical constant depending on the normalization convention for the wave function, Eq. (8), and Σ_f takes into account all the quark-scattering channel combinations. The channel index in the quark amplitudes M^m has been left implicit. $\mathscr{R}^{(f)}$ is a fourth degree homogeneous polynomial of the hadronic wave functions $\mathscr{P}$.

III. COLOR MIXING AND RANDOMIZATION

The decomposition of the color-mixing tensor U in the basis $(c_I)_{\{a'_i\}}$ defined in Eq. (13) is

$$U_{IJK} \equiv \mathrm{tr}_c(U c_I c_J c_K). \qquad (27)$$

Since the color structure of the quark amplitudes factorizes from their helicity dependence, we can readily separate the color coefficients through which each channel combination contributes to the amplitude $\mathscr{A}$ in Eq. (25) and express them in terms of the above color-mixing tensor. For the direct channel the color coefficient is

$$B_{ttt} = \mathrm{tr}_c(U C_t C_t C_t)$$
$$= A_1^3 U_{111} + A_2^3 U_{222} + 3 A_1^2 A_2 U_{112} + 3 A_1 A_2^2 U_{122}, \qquad (28)$$

for the single interchange it is

$$B_{ttu} = \mathrm{tr}_c(U C_t C_t C_u)$$
$$= A_1^2 A_2 U_{111} + A_1 A_2^2 U_{222} + (A_1^3 + 2 A_1 A_2^2) U_{112}$$
$$+ (A_2^3 + 2 A_1^2 A_2) U_{122}, \qquad (29)$$

and for double and total interchange they are

$$B_{tuu} = B_{ttu}|_{A_1 \leftrightarrow A_2}, \quad B_{uuu} = B_{ttt}|_{A_1 \leftrightarrow A_2}. \qquad (30)$$

The above expressions distinguish explicitly between the color structure of the hard scattering contained in A_1, A_2,

and the color-mixing factors U_{IJK} generated by soft gluon exchange. This distinction is important for the model we present below.

The lowest order color-mixing tensor $U^{(0)}$ has decomposition

$$U_{111}^{(0)} = U_{222}^{(0)} = 36, \quad U_{112}^{(0)} = U_{221}^{(0)} = \frac{U_{222}^{(0)}}{3}, \qquad (31)$$

which yields

$$B_{ttt}^{(0)} = B_{uuu}^{(0)} = \frac{10}{3}, \quad B_{ttu}^{(0)} = B_{tuu}^{(0)} = -\frac{2}{9}. \qquad (32)$$

Note that the single and double interchange coefficients are $(-1/15)$ times the direct or total interchange. Higher order in soft gluon exchange coefficients $B^{(n)}$ can be constructed from the perturbative expansion of U to $O(\alpha_s^n (1/\widetilde{b}_m))$. This expansion has a clear meaning in the asymptotic region $s \sim |t| \rightarrow \infty$ where the Sudakov suppression $\exp(-S)$ forces the hard scatterings close together, so that $1/\widetilde{b}_m$ can be treated as a perturbative scale [13]. Botts [8], however, finds that the onset of asymptopia where the process is dominated by these perturbative contributions occurs at very high energies, $\ln(s/s_0) \sim 8$, $s_0 = 1$ GeV^2. This suggests that at moderate energies, where measurements are available, the Sudakov suppression becomes far less effective and U is beyond perturbative control. We suggest that the effect of soft gluon exchange in this region is to decorrelate the color configurations of the constituent quarks in the initial and final states from the color configurations they have when they participate in the hard scatterings. In other words, because of strong color-mixing, the color indices of the quark lines, Fig. 3, have been randomized by U by the time they enter the hard scatterings. We build this into the formalism by requiring the color-mixing tensor U_{IJK} to be totally symmetric in the bases of Eqs. (13) and (16) and to satisfy

$$U_{111}^{\mathrm{rand}} = U_{222}^{\mathrm{rand}} = U_{112}^{\mathrm{rand}} = U_{221}^{\mathrm{rand}}. \qquad (33)$$

Compare this with Eq. (31) and note that the above relation is not assumed to be valid order by order in α_s. It is a statement about color flow in the nonperturbative regime. The color randomization condition (33) yields, via Eqs. (28)–(30),

$$B_{ttt}^{\mathrm{rand}} = B_{uuu}^{\mathrm{rand}} = B_{ttu}^{\mathrm{rand}} = B_{tuu}^{\mathrm{rand}}. \qquad (34)$$

This relation holds independently of the specific value of the hard color coefficients A_1, A_2. It means that the color structure of the short distance subprocess becomes irrelevant for the determination of the hadronic amplitude exactly because it is unstable under soft gluon exchange over large space-time scales.[1] Since all channel configurations contribute with the same color coefficients in the Landshoff mechanism, the

---

[1] Similar ideas have been suggested in the context of diffractive deep inelastic scattering (DIS) and heavy quarkonium production in Refs. [15,16], respectively.

elastic scattering will be dominated by the interchange channels as they are more numerous.

In order to demonstrate the combined effect of flavor flows and color factors without the complications of spin we consider a toy model where the constituent quarks are scalars. The quark Born amplitudes, Fig. 2, are

$$M_t = g^2 \frac{1}{t}(k_1+k_3)\cdot(k_2+k_4)(C_t)_{\{a_i\}} = g^2\left(\frac{s-u}{t}\right)(C_t)_{\{a_i\}},$$

$$M_u = g^2 \frac{1}{u}(k_1+k_4)\cdot(k_2+k_3)(C_u)_{\{a_i\}} = g^2\left(\frac{s-t}{u}\right)(C_u)_{\{a_i\}},$$

$$M_s = g^2 \frac{1}{s}(k_1-k_2)\cdot(k_3-k_4)(\bar{C}_s)_{\{a_i\}} = g^2\left(\frac{u-t}{s}\right)(\bar{C}_s)_{\{a_i\}}. \tag{35}$$

The pp and $\bar{p}p$ amplitudes are determined by simply counting the available channel combinations:

$$\mathscr{A}^{pp}_{\text{scalar}} = \frac{N}{stu}\text{tr}_c\{U[3(M_t+M_u)^3$$

$$+6(M_t^2+M_u^2)(M_t+M_u)]\}\mathscr{T}, \tag{36}$$

$$\mathscr{A}^{\bar{p}p}_{\text{scalar}} = \frac{N}{stu}\text{tr}_c\{U[3(M_t+M_s)^3$$

$$+6(M_t^2+M_s^2)(M_t+M_s)]\}\mathscr{T}. \tag{37}$$

The first term in Eq. (36) comes from the contributions of Fig. 1(a) and the second from Figs. 1(b) and 1(c). The flavor-inequivalent reorderings of the hard scatterings have been taken into account. The factor $\mathscr{T}$ contains the integrations over momentum fractions and impact parameters as in Eq. (25) and depends on the hadronic mass scales. At $\theta = 90°$, annihilation channels do not contribute ($M_s = 0$) and direct and interchange channels are equal up to their respective color structure. Then the amplitude ratio depends only on the color coefficients B:

$$\left|\frac{\mathscr{A}^{\bar{p}p}}{\mathscr{A}^{pp}}\right|_{\theta=90°} = \left|\frac{9B_{ttt}}{9B_{ttt}+9B_{uuu}+15B_{ttu}+15B_{tuu}}\right|. \tag{38}$$

At asymptotically high energies, the lowest perturbative order coefficients $B^{(0)}$ of Eqs. (32) give

$$R^{\text{as}}_{\bar{p}p}(s,\theta=90°) = \left(\frac{9}{16}\right)^2 = \frac{1}{3.16}. \tag{39}$$

At moderate energies, where color randomization is assumed to occur, the color coefficients B^{rand}, Eq. (34), yield

$$R^{\text{rand}}_{\bar{p}p}(s,\theta=90°) = \frac{1}{9}R^{\text{as}}_{\bar{p}p}(s,\theta=90°) = \frac{1}{28.4}. \tag{40}$$

Color randomization results in a smaller ratio because the interchange channels in Eq. (36) give much bigger relative

contribution to the pp amplitude than in lowest order in PQCD. In the next section we shall see that this feature of Landshoff scattering persists after the inclusion of the spin of the quarks.

IV. ELASTIC SCATTERING IN THE HELICITY BASIS

In this section we compute the baryon-baryon (pp, $\bar{p}p$, and np) elastic amplitudes for wide-angle scattering both in the asymptotic energy limit and for moderate energies, where the assumption of color randomization is believed to be relevant. According to Eq. (25) the elastic amplitude for given baryon helicities is obtained by summing over all quark-scattering channels that are allowed by helicity conservation, weighed by the appropriate wave function factors $\mathscr{R}$ and color traced after contraction with the color-mixing tensor U. For very large momentum transfer $|t|$, the dependence of the Sudakov exponent S_I on the color flow of the corresponding hard scattering enters as nonleading logarithmic dependence on t, Eq. (23). It has been argued that these nonleading logarithmic corrections can give rise to nontrivial phase structure in the amplitude that may account for its oscillatory behavior with energy [17,18]. In the following we are going to neglect them because, although our model retains the flavor and crossing structure of PQCD, it is suggested to be valid in an energy region where the perturbative expansion of radiative corrections is not applicable. In this case we will actually set the whole Sudakov exponent equal to zero.

The decomposition of the hadronic state in terms of quark helicities is given by Eq. (8). The results are given in terms of a general $\mathscr{P}_{123}$, whose explicit form is determined by considering specific models for the proton wave function [10,11]. The pp and $\bar{p}p$ amplitudes can be expressed in terms of the following five wave function combinations:

$$\mathscr{R}_0 = \mathscr{P}^4_{123} + \mathscr{P}^4_{213} + 16\mathscr{T}^4_{123} + (1\leftrightarrow3) + (2\leftrightarrow3),$$

$$\mathscr{R}_1 = 2\mathscr{P}^2_{123}\mathscr{P}^2_{213} + 8\mathscr{P}^2_{123}\mathscr{T}^2_{123} + 8\mathscr{P}^2_{213}\mathscr{T}^2_{123} + (1\leftrightarrow3)$$

$$+ (2\leftrightarrow3),$$

$$\mathscr{R}'_1 = 2\mathscr{P}^2_{123}\mathscr{P}^2_{312} + 2\mathscr{P}^2_{132}\mathscr{P}^2_{213} + 8\mathscr{P}^2_{213}\mathscr{T}^2_{132} \tag{41}$$

$$+ 8\mathscr{P}^2_{312}\mathscr{T}^2_{123} + (1\leftrightarrow2) + (1\leftrightarrow3),$$

$$\mathscr{R}'_2 = 2\mathscr{P}^2_{123}\mathscr{P}^2_{132} + 32\mathscr{T}^2_{123}\mathscr{T}^2_{132} + (1\leftrightarrow2) + (1\leftrightarrow3),$$

$$\mathscr{R}'_3 = 16\mathscr{P}_{123}\mathscr{P}_{132}\mathscr{T}_{123}\mathscr{T}_{132} + (1\leftrightarrow2) + (1\leftrightarrow3).$$

The additional terms generated by the permutations shown in the above equations are because of the flavor inequivalent relabelings of the three hard scatterings M^m. $\mathscr{R}_1$ contributes to the diagram Fig. 1(a), the three $\mathscr{R}'$'s contribute to the diagrams Figs. 1(b) and 1(c), and $\mathscr{R}_0$ contributes to all three diagrams Figs. 1(a)–1(c).

The pp helicity amplitudes are

$$\mathscr{A}^{pp}(++;++) = -\frac{N(8\pi)^3}{stu}\int_0^1\frac{dx_1dx_2}{x_1^2x_2^2x_3^3}\int d\widetilde{b}_1d\widetilde{b}_2\,\alpha_s^3(\mu)\exp(-S^1-S^2-S^3)$$

$$\times\left[B_{ttt}(2\mathscr{R}_0)\left(\frac{s^3}{t^3}+\frac{s^3}{u^3}\right)+B_{ttt}(\mathscr{R}_1+\mathscr{R}_1'+\mathscr{R}_2')\left(\frac{su^2}{t^3}+\frac{st^2}{u^3}\right)\right.$$

$$\left.+B_{ttu}(4\mathscr{R}_0)\left(\frac{s^3}{t^2u}+\frac{s^3}{tu^2}\right)+B_{ttu}(\mathscr{R}_1+\mathscr{R}_2')\left(\frac{su}{t^2}+\frac{st}{u^2}\right)\right], \tag{42}$$

$$\mathscr{A}^{pp}(+-;+-) = \frac{N(8\pi)^3}{stu}\int_0^1\frac{dx_1dx_2}{x_1^2x_2^2x_3^3}\int d\widetilde{b}_1d\widetilde{b}_2\,\alpha_s^3(\mu)\exp(-S^1-S^2-S^3)$$

$$\times\left[B_{ttt}(2\mathscr{R}_0)\frac{u^3}{t^3}+B_{ttt}(\mathscr{R}_1+\mathscr{R}_1'+\mathscr{R}_2')\frac{s^2u}{t^3}\right.$$

$$\left.+B_{ttu}(2\mathscr{R}_1+\mathscr{R}_1')\frac{s^2}{t^2}+B_{ttu}(\mathscr{R}_1+\mathscr{R}_3')\left(\frac{t}{u}+\frac{s^2}{tu}\right)\right], \tag{43}$$

and

$$\mathscr{A}^{pp}(+-;-+) = \mathscr{A}^{pp}(+-;+-)|_{t\leftrightarrow u}. \tag{44}$$

The $\bar{p}p$ helicity amplitudes are obtained from the above pp amplitudes via the following crossings:

$$\mathscr{A}^{\bar{p}p}(++;++) = \mathscr{A}^{pp}(+-;+-)|_{s\leftrightarrow u},$$

$$\mathscr{A}^{\bar{p}p}(+-;+-) = \mathscr{A}^{pp}(++;++)|_{s\leftrightarrow u}, \tag{45}$$

$$\mathscr{A}^{\bar{p}p}(+-;-+) = \mathscr{A}^{pp}(+-;-+)|_{s\leftrightarrow u}.$$

Finally, the np helicity amplitudes are given in the Appendix.

The observables we are considering here do not depend significantly on the specific form of the hadronic wave function. Model light-cone distribution amplitudes affect the overall normalization of the hadronic amplitudes because of the asymmetric distribution of the longitudinal momentum among the valence quarks [9,11]. Because of the permutations of the arguments in Eqs. (41), though, the wave function model dependence of the cross section ratios and the angular distribution is expected to be minimal [8]. Consequently, to compute $R_{\bar{p}p/pp}$ we use the totally symmetric $\mathscr{P}_{123}=\mathscr{P}_{as}$, and the above wave function combinations become

$$\mathscr{R}_0 = 54\mathscr{P}_{as}^4, \quad \mathscr{R}_1 = 54\mathscr{P}_{as}^4,$$

$$\mathscr{R}_1' = 60\mathscr{P}_{as}^4, \quad \mathscr{R}_2' = 102\mathscr{P}_{as}^4, \quad \mathscr{R}_3' = 48\mathscr{P}_{as}^4. \tag{46}$$

The above forms for the wave function combinations and Eqs. (42)–(45) reproduce the results of Farrar and Wu in Ref. [19] up to an overall normalization factor. The ratio $R_{\bar{p}p/pp}$ is given in the helicity basis by

$$R_{\bar{p}p/pp} = \frac{|\mathscr{A}^{\bar{p}p}(++;++)|^2+|\mathscr{A}^{\bar{p}p}(+-;+-)|^2+|\mathscr{A}^{\bar{p}p}(+-;-+)|^2}{|\mathscr{A}^{pp}(++;++)|^2+|\mathscr{A}^{pp}(+-;+-)|^2+|\mathscr{A}^{pp}(+-;-+)|^2}. \tag{47}$$

Using the lowest perturbative order color coefficients $B^{(0)}$ in Eq. (32), we obtain the result

$$R_{\bar{p}p/pp}^{as}(s,\theta=90°) \approx \frac{1}{2.68}. \tag{48}$$

This result, although definitely less than unity, is much larger than the experimental value $R_{\bar{p}p/pp}\approx 1/40$, measured at $\sqrt{s}=3.59$ GeV [7]. For the color randomization model, we compute $R_{\bar{p}p/pp}$ using again the asymptotic wave functions of Eq. (46), and the color factors B^{rand} of Eq. (34). The result is

$$R_{\bar{p}p/pp}^{rand}(s,\theta=90°) \approx \frac{1}{27.7}. \tag{49}$$

Color randomization yields a ratio one order of magnitude smaller than the asymptotic case and close in value to the scalar quark toy model of the previous section. The corresponding results for np elastic scattering are obtained by using the helicity amplitudes given in the Appendix:

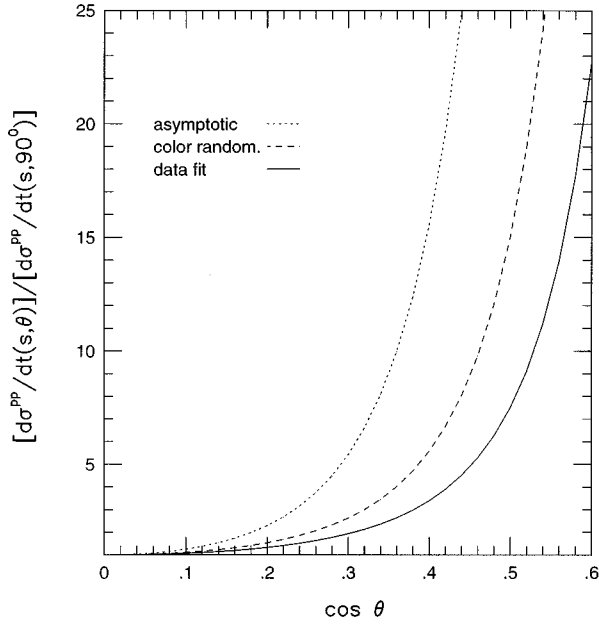$$R_{np/pp}^{as}(s,\theta=90°)\approx 0.30, \quad R_{np/pp}^{rand}(s,\theta=90°)\approx 0.36. \tag{50}$$

FIG. 4. Angular distribution for proton-proton elastic scattering. The data fit is from Ref. [19].

Color randomization gives slightly bigger ratio for np/pp elastic scattering unlike the case of $\bar{p}p/pp$. Both values of $R_{np/pp}$, though, are compatible with the experimental value [20] $R_{np/pp} = 0.34 \pm 0.05$ measured over an energy range 3.10 GeV $\leq \sqrt{s} \leq$ 4.75 GeV.

Finally, we examine the effect of color randomization on the angular distribution of pp elastic scattering. To this end we plot the differential cross section normalized at $\theta = 90°$ vs $\cos\theta$, Fig. 4. Landshoff scattering in the asymptotic limit yields a steeply rising angular distribution, approximately of the form $(1 - \cos^2\theta)^{-12}$. Color randomization softens this distribution to an approximate form $(1 - \cos^2\theta)^{-10}$. This is to be compared with the fit to the experimental data $(1 - \cos^2\theta)^{-7}$ given by Farrar and Wu in [19]. In all cases the angular distribution is independent of the c.m. energy. The color randomization distribution is in relatively good agreement with the experimental fit for $\cos(\theta) \lesssim 0.3$ but it becomes much steeper away from the central region.

V. SUMMARY

We have considered wide-angle elastic scattering in the Landshoff mechanism and organized the calculation making explicit the effect of color. For scattering at moderate energies we have suggested a PQCD-motivated model which realizes the observation that the elastic scattering is dominated by quark interchange among the hadrons. This is assumed to occur because the color of the constituent quarks is totally randomized by soft gluon exchange. By implementing this in the expressions for the hadronic helicity amplitudes we obtain a cross section ratio $R_{\bar{p}p/pp}$ which is an order of magnitude smaller than the asymptotic value and compatible with the experimental measurements [6,7]. This feature of $R_{\bar{p}p/pp}$ is because of the nature of the Landshoff mechanism. Because in this picture the elastic process occurs via independent quark scattering, a change in the relative contribution between channels at the quark level has a sizable effect in the hadronic cross section. Color randomization leads to softening of the angular distribution in pp scattering, although we found that away from the central region it is still steeper than what experiment suggests.

On the theoretical side, the separation of gluons into hard and soft becomes less clear away from asymptopia, because of the small momentum transfers involved. Moreover, conservation of color and color randomization require to include components of the hadronic wave function beyond the leading twist three-quark part. Another set of approximations we made has to do with helicity conservation. In the moderate energy regime, quark mass and intrinsic transverse momentum corrections can be important. This is the reason why we did not reproduce the $\sim s^{-10}$ scaling of the elastic cross section. We considered instead observables which are less sensitive to the specific form of the hadronic wave function or the factorization assumptions and mainly determined by the flavor routing of the constituent quarks. Cross section ratios involving meson scattering, where data are also available, are currently under study. Moreover, it would be of interest to analyze the contribution of the Landshoff mechanism relative to the QIM mechanism, as in Ref. [21], by taking into account color randomization.

ACKNOWLEDGMENTS

APPENDIX

Because of isospin symmetry the wave function for the neutron is obtained from the corresponding one for the proton via the substitution $u \rightarrow -d$ and $d \rightarrow u$ in Eqs. (7) and (8). For np elastic scattering, apart from the wave function combinations given in Eq. (42), an additional one is needed: namely,

$$\mathscr{R}'_4 = 8\mathscr{P}_{123}\mathscr{P}_{213}\mathscr{P}_{312}\mathscr{T}_{132} + 8\mathscr{P}_{132}\mathscr{P}_{312}\mathscr{P}_{213}\mathscr{T}_{123} + (1 \rightarrow 2)$$

$$+ (1 \rightarrow 3). \tag{A1}$$

The np helicity amplitudes are

$$\mathscr{A}^{np}(++;++) = -\frac{N(8\pi)^3}{stu} \int_0^1 \frac{dx_1 dx_2}{x_1^2 x_2^2 x_3^3} \int d\tilde{b}_1 d\tilde{b}_2 \alpha_s^3(\mu) \exp(-S^1 - S^2 - S^3)$$

$$\times \left[B_{ttt}(2\mathscr{R}_0)\left(\frac{s^3}{t^3} + \frac{s^3}{ut^2} + \frac{s^3}{tu^2}\right) + B_{ttt}(\mathscr{R}_1 + \mathscr{R}'_1 + \mathscr{R}'_2)\frac{su^2}{t^3} + B_{ttu}\mathscr{R}'_1\frac{su}{t^2} + B_{ttu}(2\mathscr{R}'_3)\frac{st}{u^2} \right], \tag{A2}$$

$$\mathscr{A}^{np}(+-;+-) = \frac{N(8\pi)^3}{stu}\int_0^1 \frac{dx_1 dx_2}{x_1^2 x_2^2 x_3^3}\int d\widetilde{b}_1 d\widetilde{b}_2 \alpha_s^3(\mu)\exp(-S^1-S^2-S^3)$$

$$\times\left[B_{ttt}(2\mathscr{R}_0)\frac{u^3}{t^3} + B_{ttt}(\mathscr{R}_1+\mathscr{R}_1'+\mathscr{R}_2')\frac{s^2 u}{t^3}\right. \tag{A3}$$

$$\left. + B_{ttu}(\mathscr{R}_1'+2\mathscr{R}_2')\frac{s^2}{t^2} + B_{ttu}(\mathscr{R}_2'+\mathscr{R}_3')\left(\frac{s^2}{tu}+\frac{t}{u}\right)\right], \tag{A4}$$

and

$$\mathscr{A}^{np}(+-;-+) = -\frac{N(8\pi)^3}{stu}\int_0^1 \frac{dx_1 dx_2}{x_1^2 x_2^2 x_3^3}\int d\widetilde{b}_1 d\widetilde{b}_2 \alpha_s^3(\mu)\exp(-S^1-S^2-S^3)B_{ttu}\mathscr{R}_4'\left(2\frac{s^2}{u^2}+\frac{s^2}{tu}+\frac{u}{t}\right). \tag{A5}$$

---

[1] S. J. Brodsky and G. P. Lepage, in *Perturbative Quantum Chromodynamics*, edited by A. H. Mueller (World Scientific, Singapore, 1989).

[2] G. R. Farrar and F. Neri, Phys. Lett. **130B**, 109 (1983); **152B**, 443 (1985).

[3] J. F. Gunion, S. J. Brodsky, and R. Blankenbecler, Phys. Rev. D **8**, 287 (1973); D. Sivers, S. J. Brodsky, and R. Blankenbecler, Phys. Rep. C **23**, 1 (1976).

[4] P. V. Landshoff, Phys. Rev. D **10**, 1024 (1974); A. Donnachie and P. V. Landshoff, Z. Phys. C **2**, 55 (1979).

[5] G. P. Ramsey and D. Sivers, Phys. Rev. D **45**, 79 (1992); **47**, 93 (1993).

[6] G. C. Blazey *et al.*, Phys. Rev. Lett. **55**, 1820 (1985); B. R. Baller *et al.*, *ibid.* **60**, 1118 (1988); A. Carrol *et al.*, *ibid.* **61**, 1698 (1988).

[7] C. White *et al.*, Phys. Rev. D **49**, 58 (1994).

[8] J. Botts, Nucl. Phys. **B353**, 20 (1991).

[9] V. L. Chernyak and A. R. Zhitnitsky, Phys. Rep. **112**, 173 (1984).

[10] M. G. Sotiropoulos and G. Sterman, Nucl. Phys. **B425**, 489 (1994).

[11] V. L. Chernyak and I. R. Zhitnitsky, Nucl. Phys. **B246**, 52 (1984); I. R. Zhitnitsky, A. A. Ogloblin, and V. L. Chernyak, Yad. Fiz. **48**, 841 (1988) [Sov. J. Nucl. Phys. **48**, 536 (1988)]; I. D. King and C. T. Sachrajda, Nucl. Phys. **B279**, 785 (1987); M. Gari and N. G. Stefanis, Phys. Rev. D **35**, 1074 (1987).

[12] R. Gastmans and T. T. Wu, *The Ubiquitous Photon* (Clarendon, Oxford, 1990).

[13] J. Botts and G. Sterman, Nucl. Phys. **B325**, 62 (1989).

[14] A. H. Mueller, Phys. Rep. **73**, 237 (1981).

[15] W. Buchmüller and A. Hebecker, Phys. Lett. B **355**, 573 (1995).

[16] J. F. Amundson, O. J. P. Éboli, E. M. Gregores, and F. Halzen, Madison Report No. MADPH-95-919, 1995 (unpublished).

[17] B. Pire and J. P. Ralston, Phys. Lett. **117B**, 233 (1982).

[18] C. E. Carlson, M. Chachkhunashvili, and F. Myhrer, Phys. Rev. D **46**, 2891 (1992).

[19] G. R. Farrar and C.-C. Wu, Nucl. Phys. **B85**, 50 (1975).

[20] J. L. Stone *et al.*, Phys. Rev. Lett. **23**, 1315 (1977); **23**, 1317 (1977).

[21] G. P. Ramsey and D. Sivers, Phys. Rev. D **52**, 116 (1995).